COMP 4900A Final Project: Simulation of Quantum Tunneling Through a Double Well Barrier

Dan Griffith - 101111722
Cole McLaren - 101245922

Abstract

The simulation of this quantum tunneling has been done before in two-qubit and three-qubit systems as described in the papers *"Experimental Simulation of Quantum Tunneling in Small Systems"* by Guan-Ru Feng et al. and *"Quantum Simulation of Tunneling in Small Systems"* by Andrew T. Sornborger. Using this previous work, we have expanded this to a scalable system that can use more qubits. In this paper, we will discuss the results of scaling this system to 4 qubits. The introduction of more qubits introduces a higher level of resolution in representing energy waves linearly and increases the total number of measurements that the simulation can take exponentially. This larger space also allows for greater variability in the location of where the double well potential can be placed in the simulation.

Introduction/Background

In classical mechanics, a particle confined within a potential well is restricted by energy conservation: it cannot access regions where the potential energy exceeds its total energy (University of Texas at Austin, n.d.). However, in quantum mechanics, particles can tunnel through classically forbidden regions due to the probabilistic nature of the wave function. This phenomenon, known as quantum tunneling, is central to a wide range of physical systems—from electron transport in semiconductors to the behavior of magnetic nanoparticles at low temperatures.

The modeling of this behavior is possible using quantum circuits. Previous experiments conducted by Feng et al. (2013), simulate the kinetic evolution operator using single qubit $\mathbf{Z}$ rotations and multi-qubit interaction ϕ phases (Feng et al., 2013). These two operators play a specific role in the overall representation of the energy state evolution. These off-diagonal couplings model quantum tunneling and oscillation of a particle in potential wells. The constructed Q gate acts as the potential energy operator and applies the energy term in the Hamiltonian to simulate the barrier (Feng et al., 2013).

By measuring the overlap of the evolved energy wavefunction in different basis states, we can observe the probability distribution shift that signals tunneling. This shift is governed by the underlying eigenvalue spectrum derived from the Hamiltonian rotation measurement. These eigenvalues dictate the phase accumulation during the system's evolution over time. The separation of these eigenvalues illustrates tunneling rates and energy splitting (Rodríguez-Sotelo & Kozuch, 2025).

In this paper, we have taken the 2 and 3 qubit design developed by Feng et al. (2013) and expanded it to a 4 qubit system. Expanding the system to 4 qubits exponentially increases the number of measurements that can be taken, along with a linearly scaling ability to explain the energy dynamics of the system.

Methods

1 - Qubit Representation and Position Encoding

Our simulation utilizes a four-qubit register, allowing us to represent $2^4 = 16$ discrete spatial positions along a one-dimensional quantum lattice. Each computational basis state from |0000> to |1111> uniquely corresponds to a point on this lattice. For example, |0000⟩represents the leftmost position (position 0), while |1111> corresponds to the rightmost point (position 15). This encoding enables the simulation of particle localization, propagation, and tunneling across a discrete spatial region.

This approach aligns with common practices in quantum simulation, where qubits encode spatial information, and the evolution of the wavefunction over time models the physical dynamics of quantum systems (Lloyd, 1996).

2 - Circuit Construction

To simulate the evolution of a quantum particle within a potential energy landscape, we construct a time-evolution circuit that applies four primary operations during each discrete time step. These are applied in sequence and then repeated over many iterations (steps) to simulate dynamical behavior governed by the time-dependent Schrödinger equation (Griffiths, 2018). The structure of each timestep is as follows:

3 - Quantum Fourier Transform (QFT)

The circuit begins each time step with the application of a Quantum Fourier Transform (QFT). The QFT maps the quantum state from the position basis to the momentum basis. This transformation is important because kinetic energy operators (related to momentum) are diagonal in the momentum basis, making them straightforward to implement as phase rotations (Rioux, n.d.). Without this transformation, it would be significantly more complex to simulate kinetic evolution directly on a position basis.

4 - D-Gate: Momentum Evolution Operator

Following the QFT, we apply the D-Gate — a diagonal unitary matrix that encodes the momentum evolution of the quantum system. The D-Gate is constructed in the same way as in the experiment done by Feng et al. (2013), only the system has been expanded to 4 qubits.

- **Z-gate Contributions:** Each qubit contributes a single-qubit Z rotation term that corresponds to its momentum energy. The scaling factors for these terms are based on the discretized kinetic energy operator, where qubits representing higher momentum receive proportionally larger phase shifts. While Z gates do not generate superposition by themselves, they apply phase rotations to the |1⟩ component of a qubit. When the system is in superposition (as it is after the QFT), these Z-phase contributions become critical: they rotate components of the quantum state differently, setting up constructive and destructive interference that drives the system's dynamics across basis states.
- **Φ-gate (Phi) Contributions:** To more accurately capture the interaction between qubit pairs and simulate second-order effects, we include pairwise Φ gates. These two-qubit diagonal phase operations represent momentum cross-terms (i.e., coupling between different momentum components) and are essential for more precise kinetic energy modeling in a multi-qubit setting. Importantly, when applied to qubits in superposition, the Φ gates can introduce **quantum**

entanglement, as they apply conditional phase shifts based on the joint state of two qubits. This interaction cannot be decomposed into independent single-qubit operations and thus creates quantum correlations between qubit pairs that persist throughout the simulation.

The full resulting D-Gate is therefore a 16×16 diagonal unitary matrix applied simultaneously to all basis states, with each diagonal entry calculated based on the binary state's qubit values and the combined kinetic phase shift it should accrue during the timestep. Together, the Z and Φ components simulate how a quantum particle's wave function disperses and interferes under momentum dynamics in a discretized quantum system.

5 - Inverse QFT

After momentum evolution, we apply the inverse QFT to return the quantum state to the position basis. This step ensures that all subsequent operations (such as potential energy interactions) occur in the spatial domain, allowing us to model localized potential barriers, wells, or harmonic landscapes.

6 - Q-Gate: Position-Space Potential Operator

Finally, the Q-Gate applies a diagonal unitary operator representing the potential energy landscape of the system. Each position on the lattice is assigned a scalar potential value V(x), and the corresponding basis state receives a phase rotation of the form $exp^{(-iV(x)*\Delta T)}$. This transformation is essential for modeling physical barriers, wells, or more complex spatial potential structures such as double wells or harmonic oscillators. As previously done on 2 and 3 qubit systems by Feng et al. (2013), we have expanded this to a 4 qubit system.

In our simulations, we have tested a variety of potential configurations, including:

- Square barriers (with high V values over a localized region),
- Double well potentials (modeled using $V(x) = a(x^2 - b^2)^2$, and
- Smooth Gaussian-like hills

Both the Q and D gates are implemented as custom Diagonal gates in Qiskit, allowing for compact and efficient simulation of their effects without decomposing them into lower-level gate sets. This also ensures exact phase accuracy for evolution over long timesteps

7 - Initialization and Simulation Execution

The simulation begins with a user-defined initial quantum state. We initialize the system in a computational basis state such as |0011>, representing a particle localized on the left of the 1D lattice. In some trials, we initialize the system in the middle of the barrier—typically as a basis state like |0111> or |1000>—to study how a particle behaves when placed at the peak of the potential energy. This models a scenario where the particle starts in a classically forbidden region and allows us to observe whether it will tunnel symmetrically into either of the adjacent wells, remain trapped, or disperse in a nontrivial pattern depending on the barrier width and potential landscape.

The quantum circuit for a single time step is constructed as described and then composed repeatedly to simulate time evolution. This is done using Qiskit's .compose() method, allowing us to simulate up to 500 or more discrete time steps depending on the desired resolution and the rate of system evolution. Smaller

values of the time increment Δt, such as 0.01, are used to achieve smoother and more realistic results over longer periods.

After completing the evolution, the final quantum state is retrieved using Qiskit's Statevector class and visualized as a probability distribution over the 16 basis states. In some visualizations, we also overlay the scaled potential energy function onto the same plot to provide an intuitive sense of how the wave function has interacted with the potential landscape.

8 - Simulation Overview

To investigate quantum tunneling dynamics, we executed a time-dependent simulation using a four-qubit quantum circuit that evolves a wavefunction across a discrete one-dimensional lattice of 16 discrete positions. Each basis state from |0000> to |1111> corresponds to a unique spatial point, allowing us to see the spread of probability over time and its interaction with varying potential energy landscapes. The system evolves under the influence of a double-well potential, using a time step size of Δt = 0.01 over 200 total iterations (steps). These parameters were used to ensure sufficient resolution for detecting slow tunneling behavior.

This state corresponds to position 3 on the lattice, placing our particle on the left side of the central potential barrier in our double-well configuration. By starting the particle here, we simulate a scenario where a quantum particle is initially confined in the left well, and observe whether, and how, it tunnels through the central barrier toward the right well over time.

This simulation uses a quantum circuit that models the time evolution of the system. This circuit represents a single time step, and each step is made up of the following stages:

1) **Quantum Fourier Transform (QFT):** Converts the quantum state from a position space to momentum space, allowing for the application of the kinetic energy operator, which is diagonal in the momentum basis.
2) **D-Gate (Momentum Evolution Operator):** A diagonal unitary operator that applies kinetic energy evolution through both individual Z-phase shifts (for each qubit) and two-qubit Φ-phase shifts (for each qubit-pair). These components work together to simulate how a wavefunction spreads or interferes based on its momentum.
3) **Inverse QFT:** Converts the quantum state back from momentum space to position space, preparing it for application of the potential
4) **Q-Gate (Potential Energy Operator):** Applies a diagonal operator encoding the position-dependent potential energy, modeled by a double well potential of the form: $V(x) = a(x^2 - b^2)^2$.

We used the parameters a = 50 and b = 0.5, applied over 16 evenly spaced points between -1 and 1, to simulate a double-well potential with a central barrier.

This single time-step circuit is then composed repeatedly–up to 500 steps in our final test– using .compose() from Qiskit. We chose a small time increment Δt = 0.01 to ensure high-resolution, stable evolution over longer durations. This repeated application of the evolution circuit allows us to observe how the initially localized particles diffuse, reflect, or tunnel based on the shape and height of the barrier.

After evolution, the final quantum state is analyzed using Qiskit's Statevector class. We take the position-space probability distribution by squaring the magnitude of the final amplitudes in each basis state. We also overlay the scaled potential energy curve V(x) on the resulting plots to visually correlate the behavior of the wavefunction with the structure of the potential.

This setup allows us to not only study the quantum tunneling phenomena, but also how the barrier width, barrier height, and initial localization affect particle propagation in discretized quantum systems.

The phase factor in our Z gates can be modeled as:

$$n = \#\ of\ qubits$$
$$k = Position\ of\ current\ qubit$$
$$Z_k = e^{(i * \frac{\pi^2}{2^{2n-1}})}$$

The phase factor in our Φ gates can be modeled as:

$$k = Position\ of\ current\ qubit$$
$$\Phi_k = e^{(i * \frac{\pi^2}{2^k})}$$

The combination of these gates as previously discussed in Methods section 1.4 for the momentum evolutionary operator labeled as gate D in **Figure 1.** These gates are modeled similarly to the gates seen in the experiment done by Feng et al. (2013).

Figure 1.

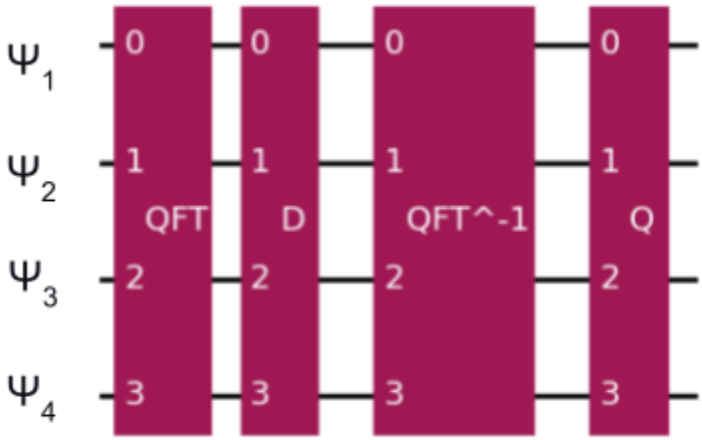

Results:

To investigate quantum tunneling behavior, we conducted a series of simulation experiments. Each experiment tested a different combination of initial quantum state and potential energy configuration to explore how particles behave in various quantum mechanical scenarios.

We began with a flat potential to establish a baseline, confirming free propagation of the wave function without barriers. We then introduced a double-well potential using a quartic function and tested several initial states: a localized particle in one well, a symmetric superposition across both wells and a fully delocalized equal superposition across all positions. Finally, we varied the barrier height by adjusting the amplitude of the potential function to observe how tunneling dynamics change with increasing energy constraints.

The following figures summarize the probability distributions over time for each scenario, providing visual confirmation of tunneling effects, interference patterns, and energy-driven localization. These experiments collectively demonstrate the quantum mechanical principles of tunneling, coherence, and the role of potential landscapes in shaping particle dynamics.

The initial state is set to |0000> with a Δ t = 0.01. The potential is held constant across all 16 basis states, simulating a flat energy landscape with no barrier or wells. As expected, the particle distributes over time, becoming more symmetric as more steps are taken (Figure 2 - 5).

Figure 2.

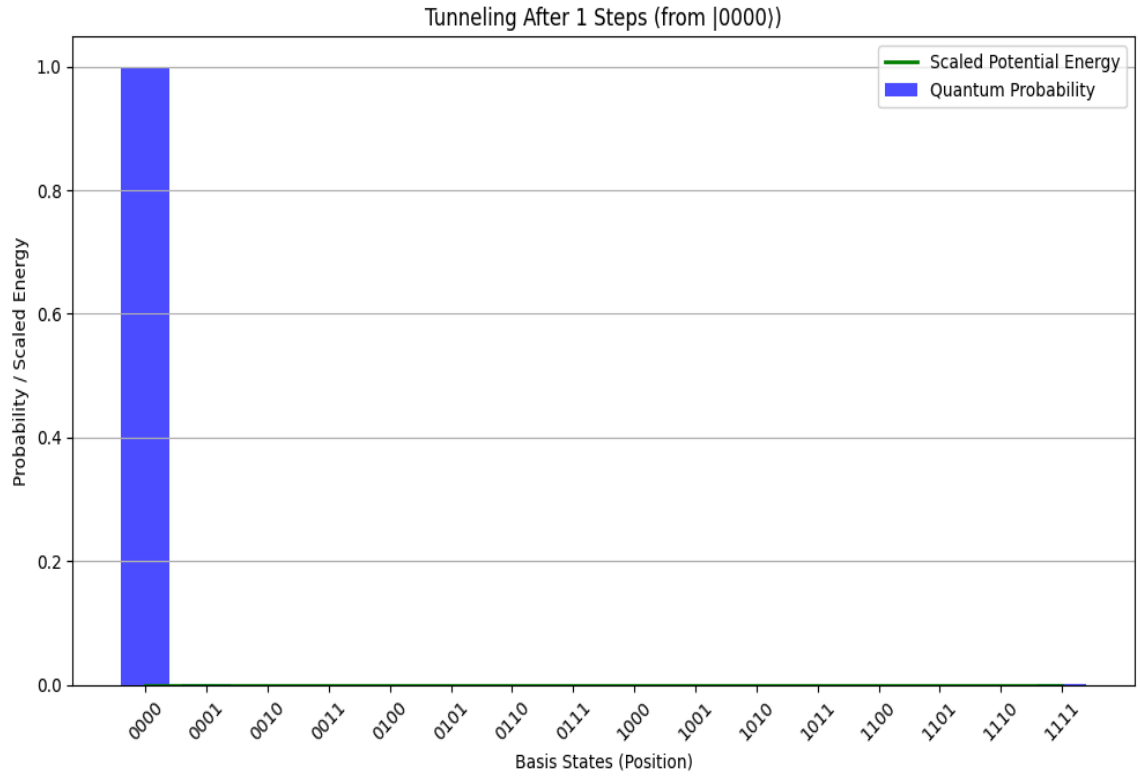

Figure 3.

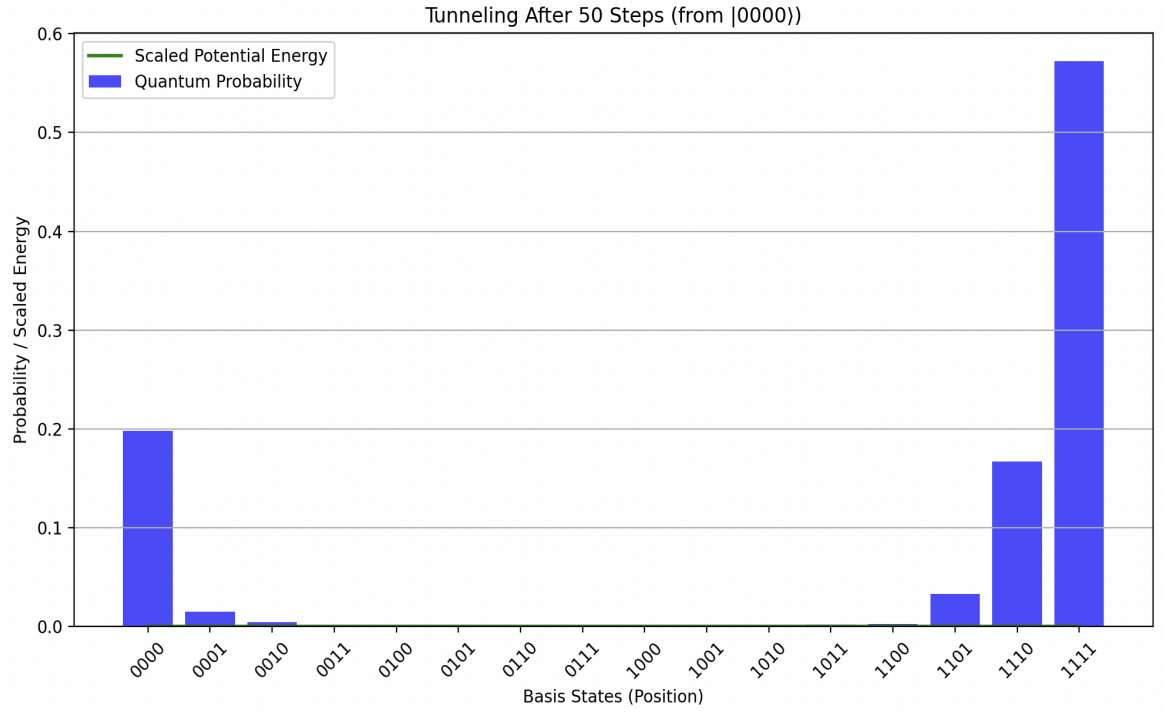

Figure 4.

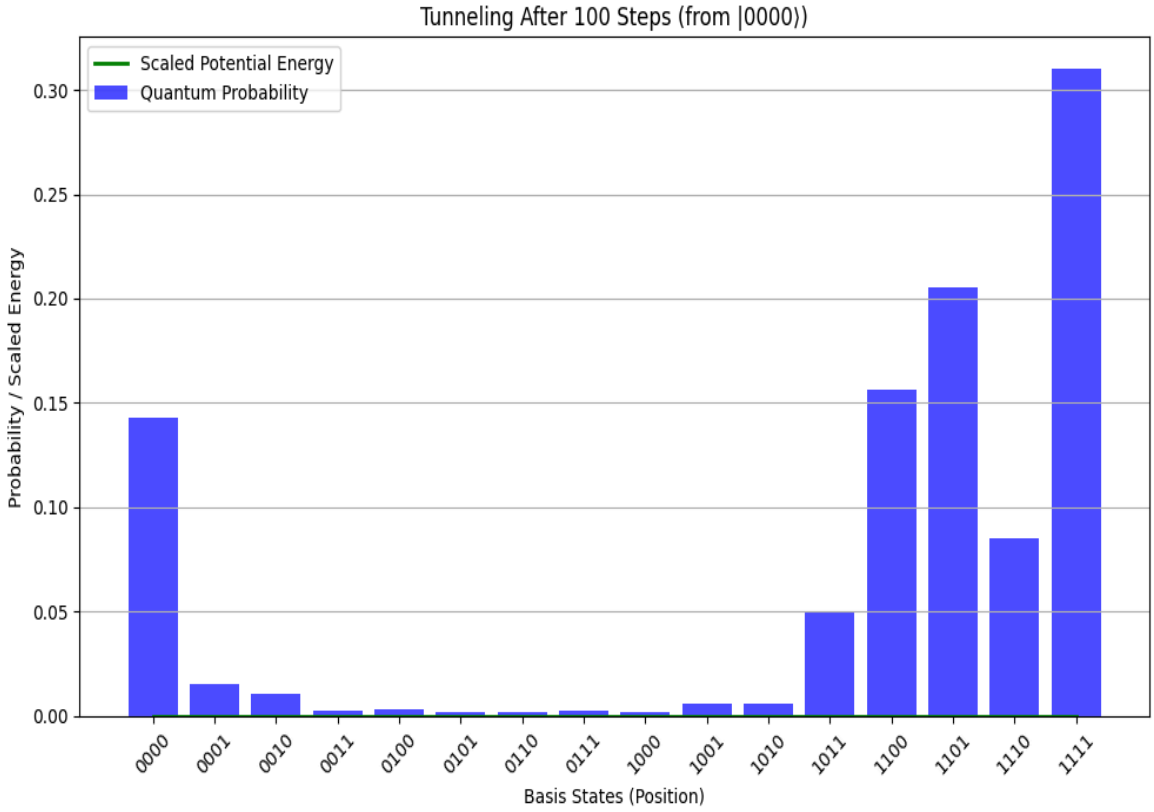

Figure 5.

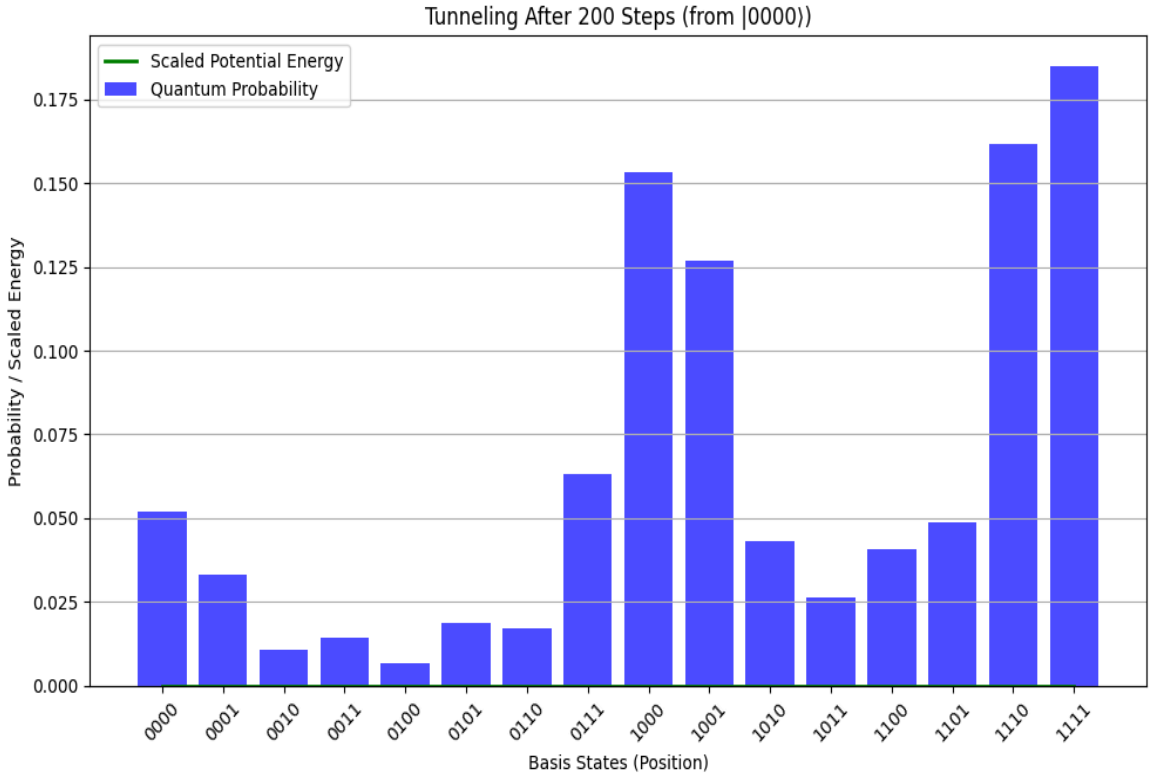

The initial state for this simulation is at |0011> with a $\Delta t = 0.01$. The probability shift shows that a localized state migrates from the left well to the right well over 200 time steps (Figure 6 - 9).

Figure 6.

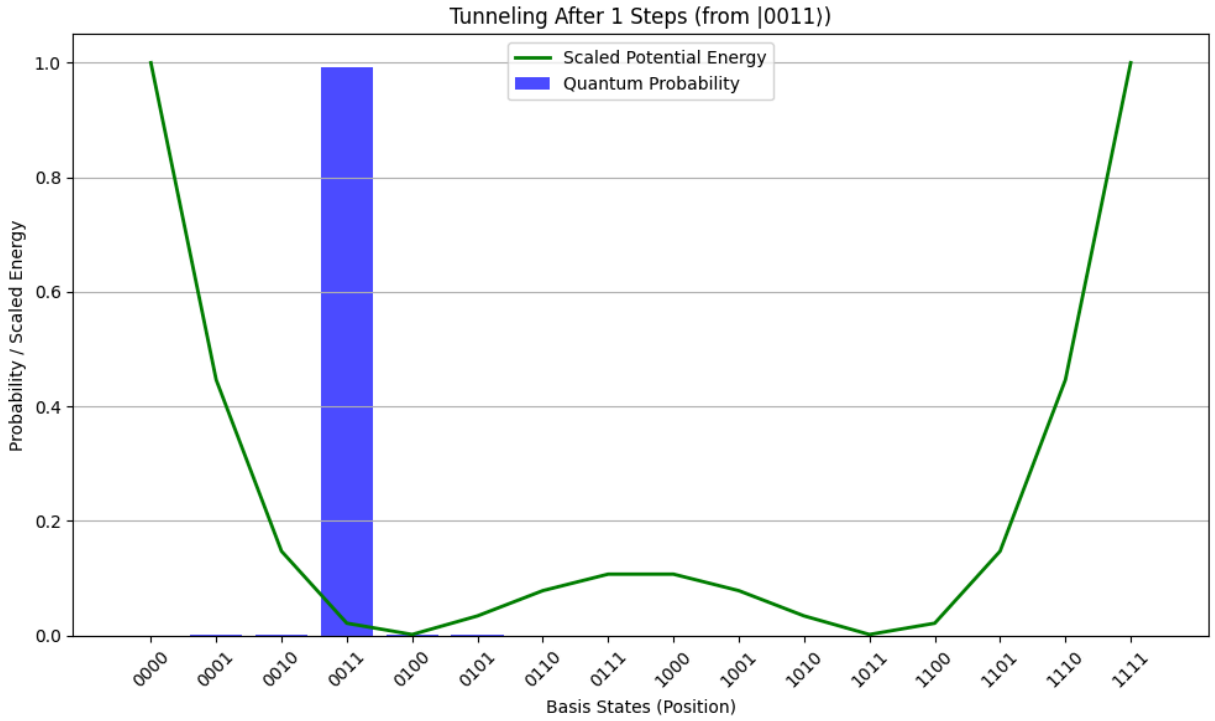

Figure 7.

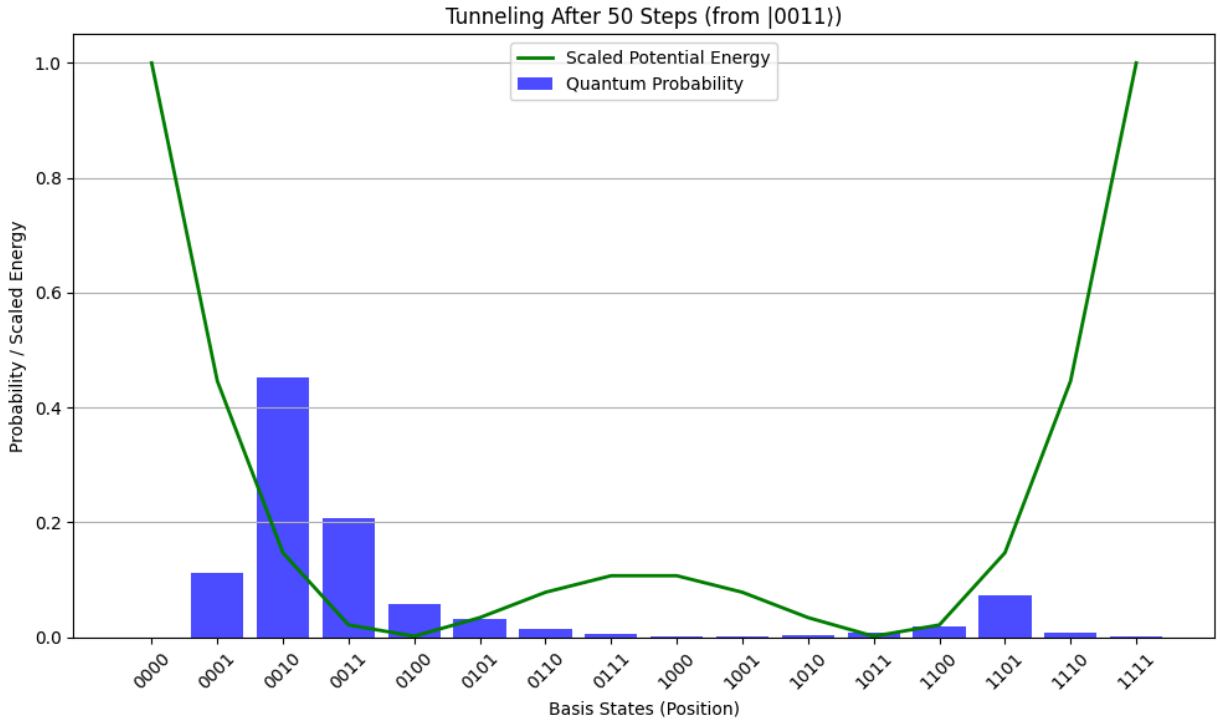

Figure 8.

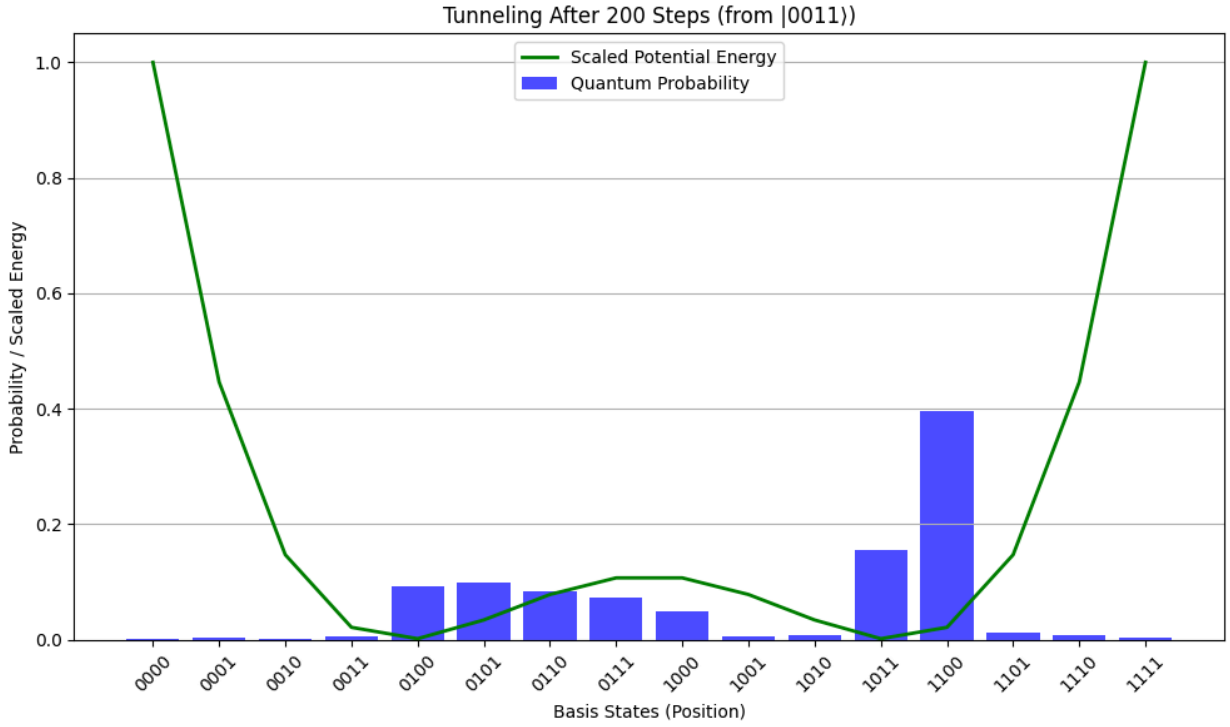

Figure 9.

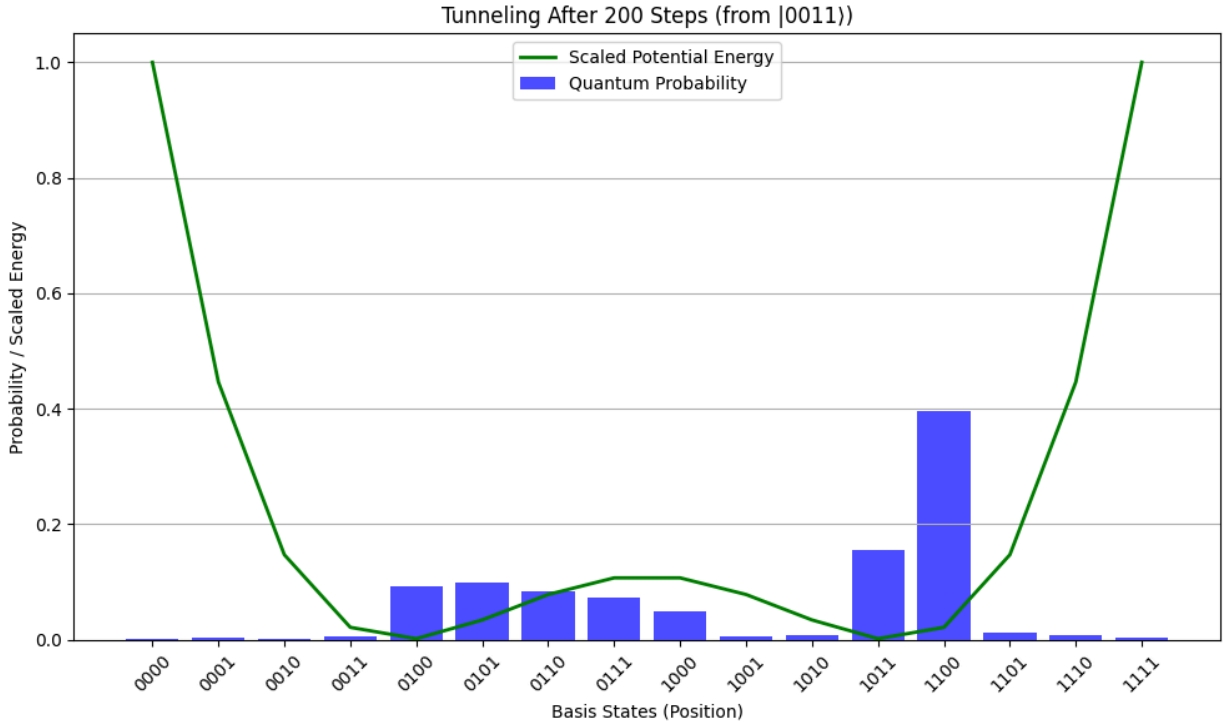

The initial state for this system is 1/√2 |0011⟩ + 1/√2 |1100⟩(left/right superposition). We can see the probabilities spread out over Δt and tunnel between the wells (Figure 10 - 13).

Figure 10.

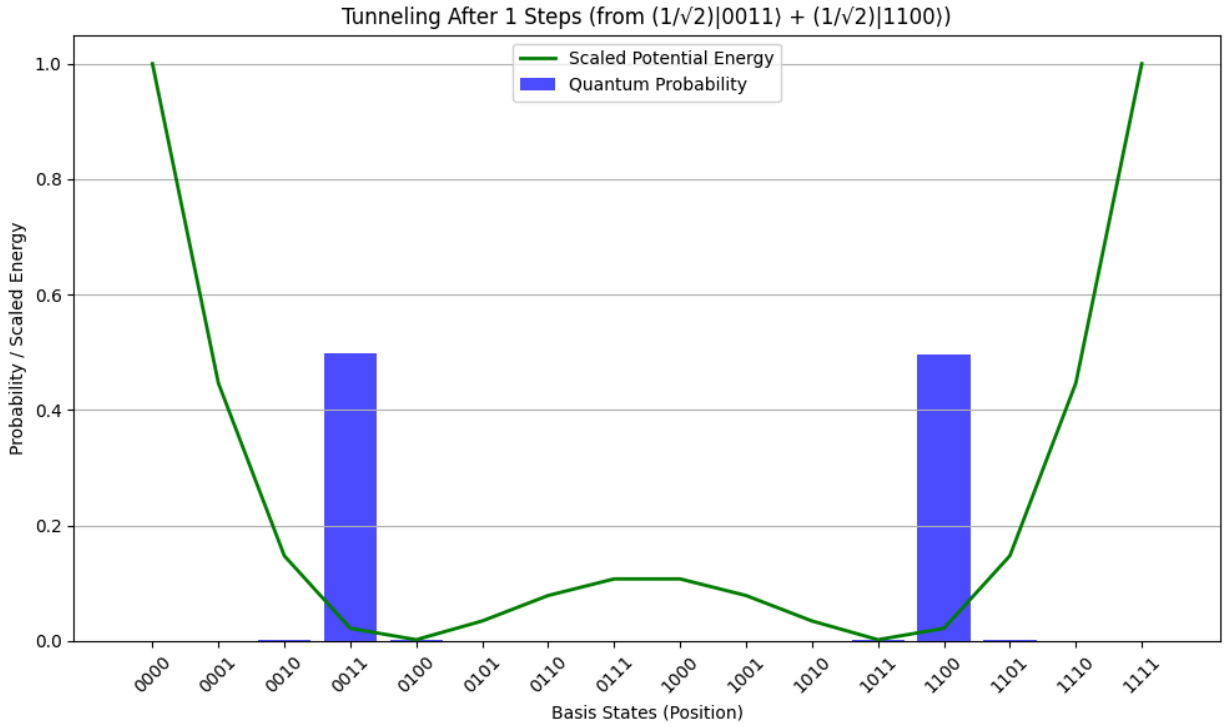

Figure 11.

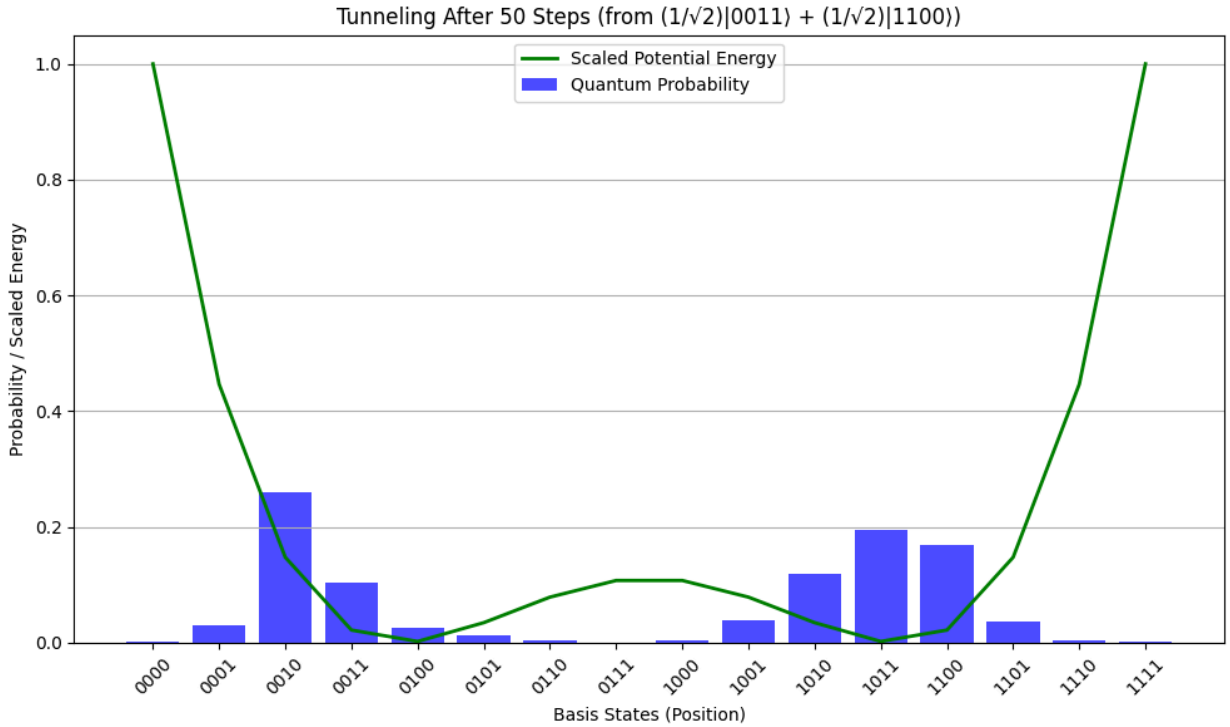

Figure 12.

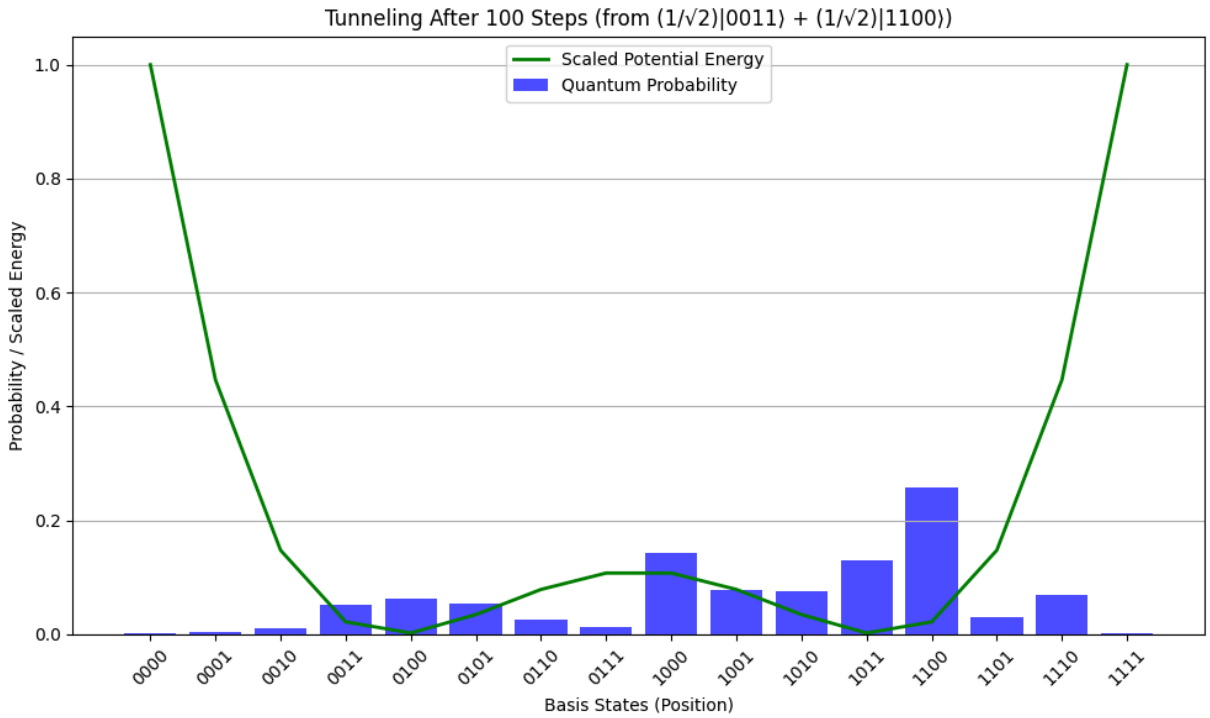

Figure 13.

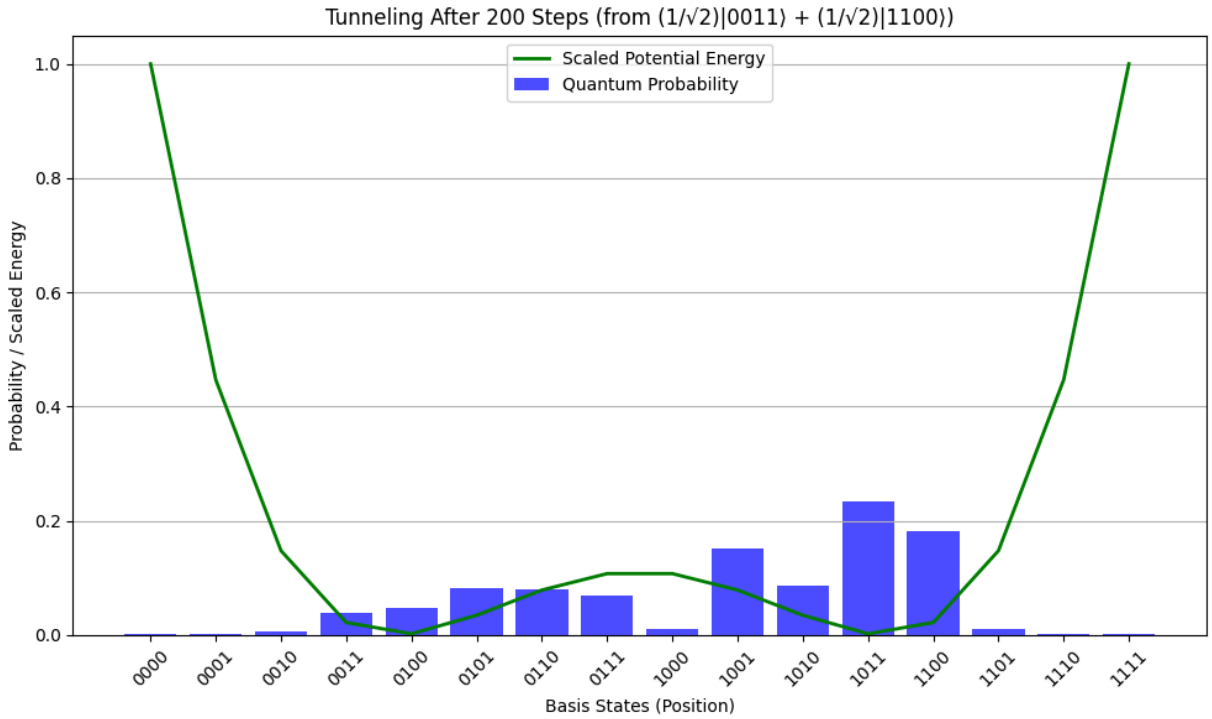

The system is initialized in an equal superposition across all 16 basis states, with Δt = 0.01. This represents a completely delocalized wave function spanning the entire spatial grid. Probability density accumulates in the two well regions over time (Figure 14 -17).

Figure 14.

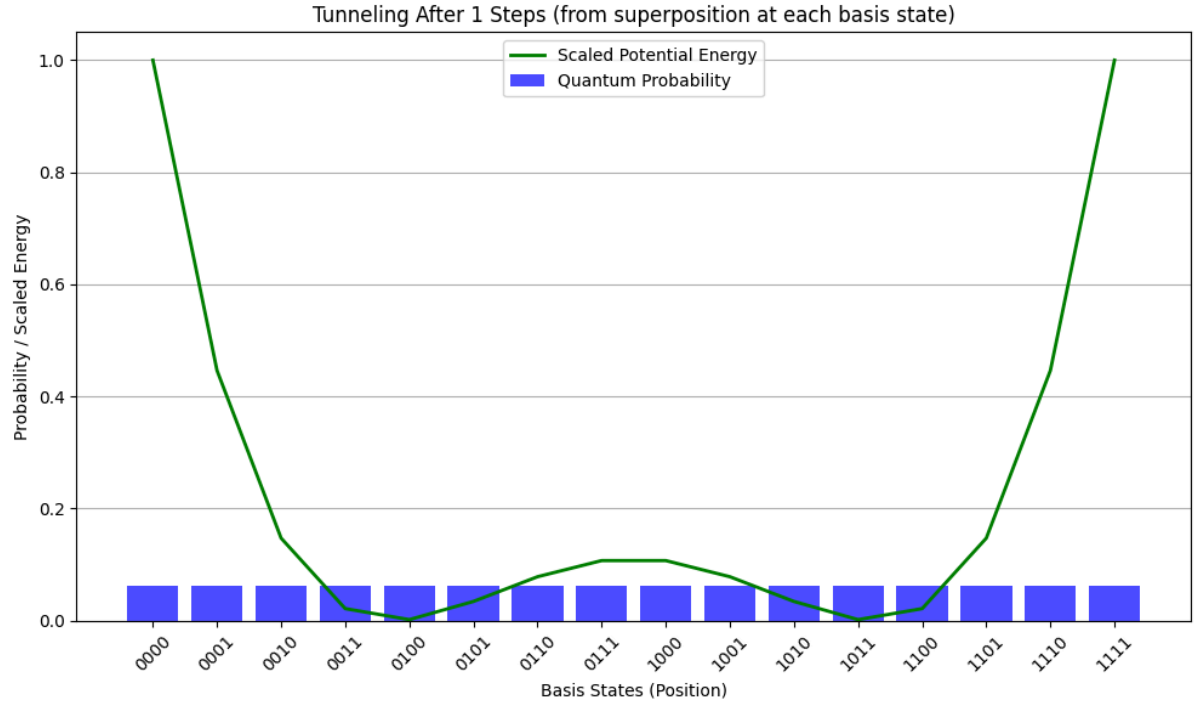

Figure 15.

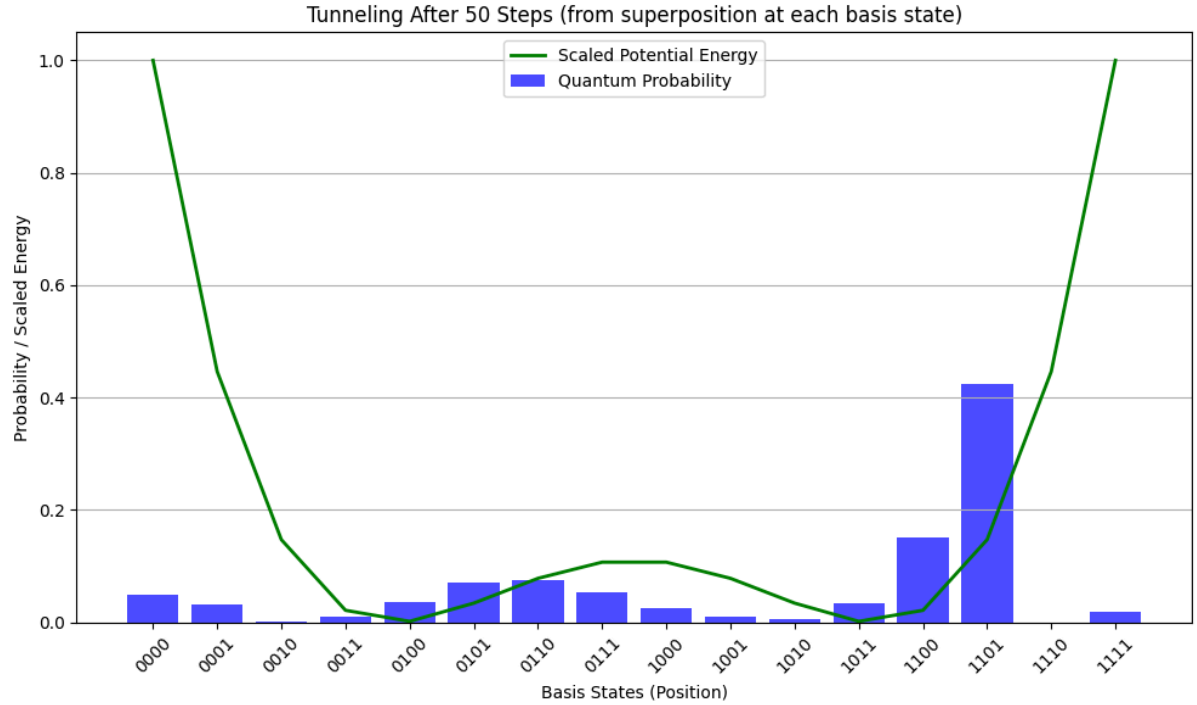

Figure 16.

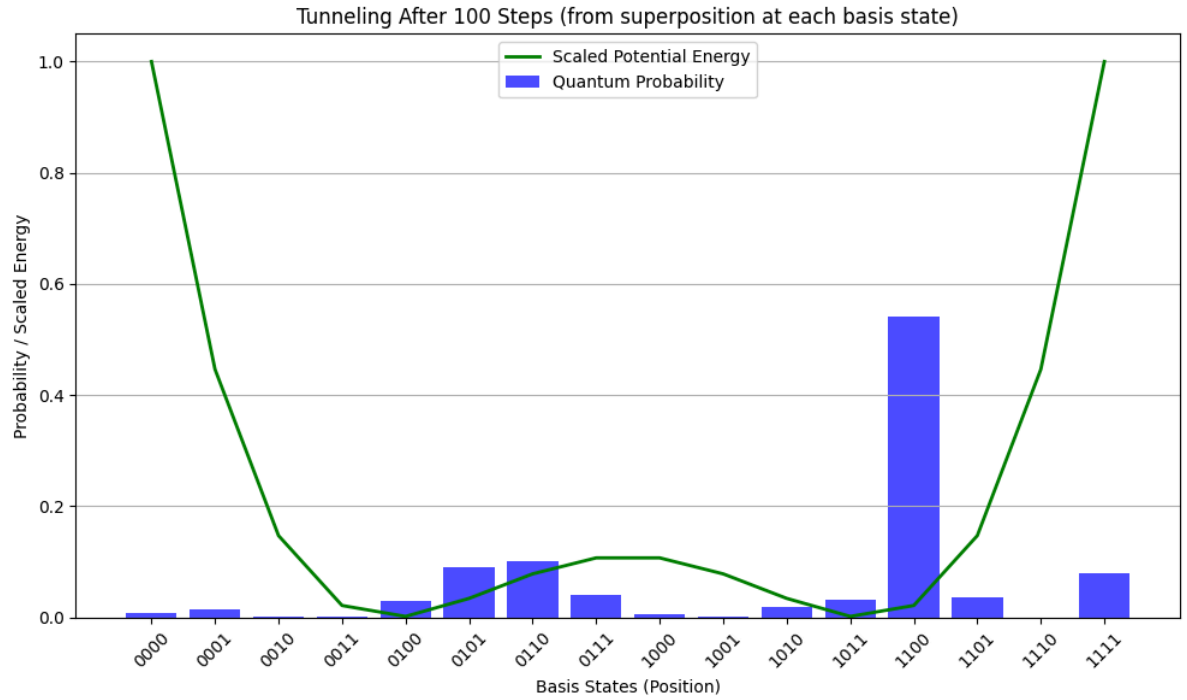

Figure 17.

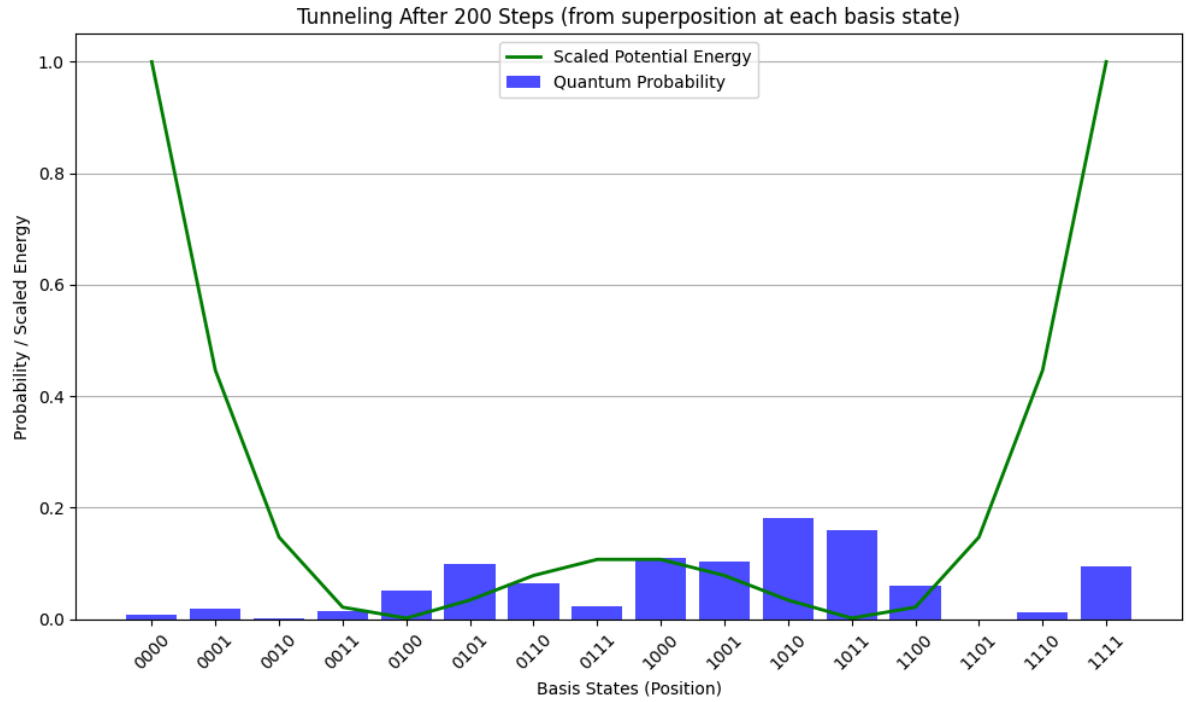

When we change the amplitude from 50 to 50,000, we can see how tunneling distributions are changed (Figure 18 - 21).

Figure 18.

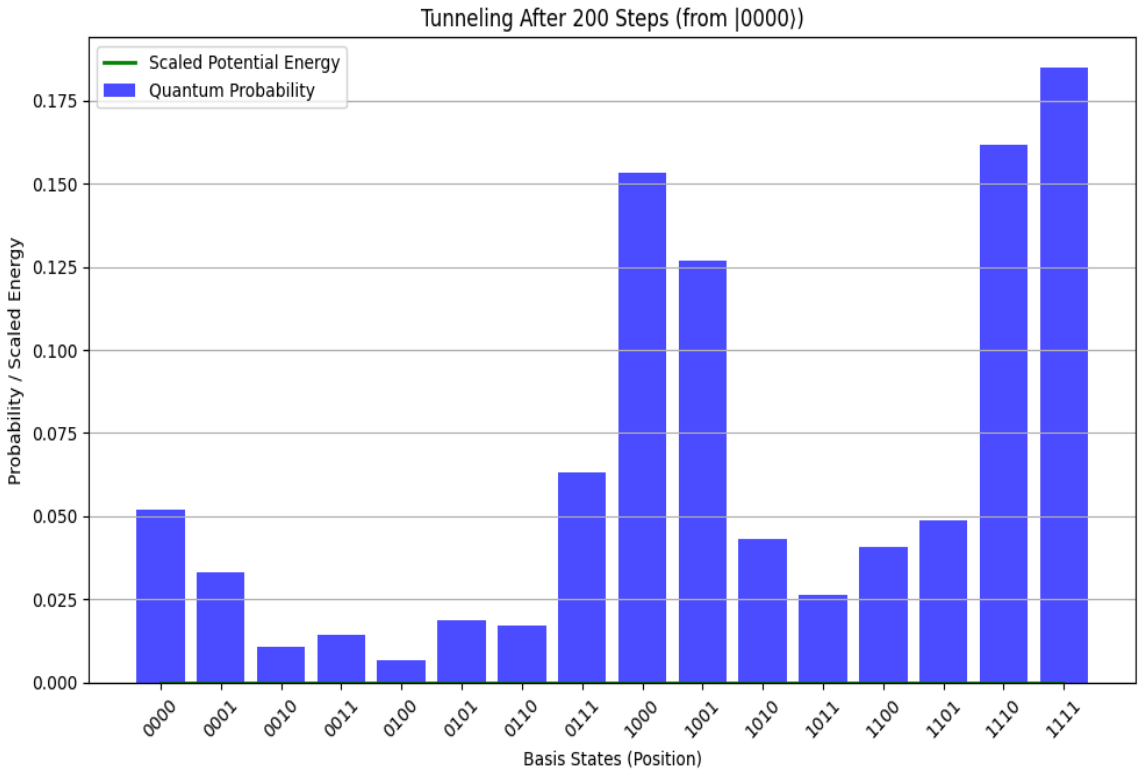

Figure 19.

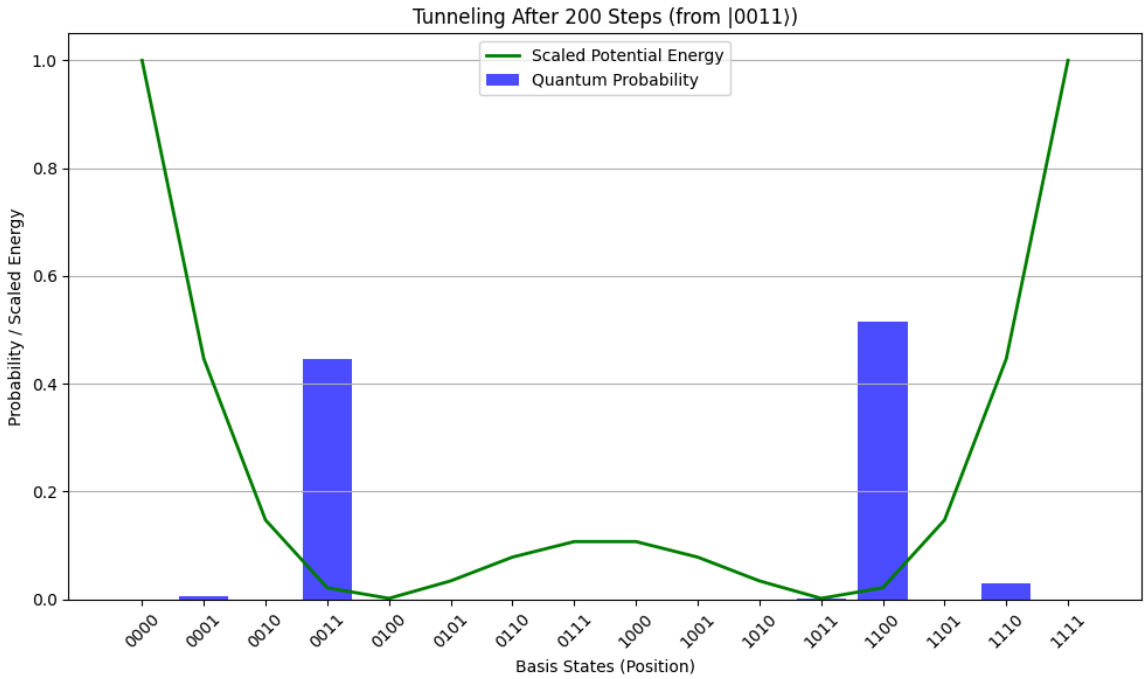

Figure 20.

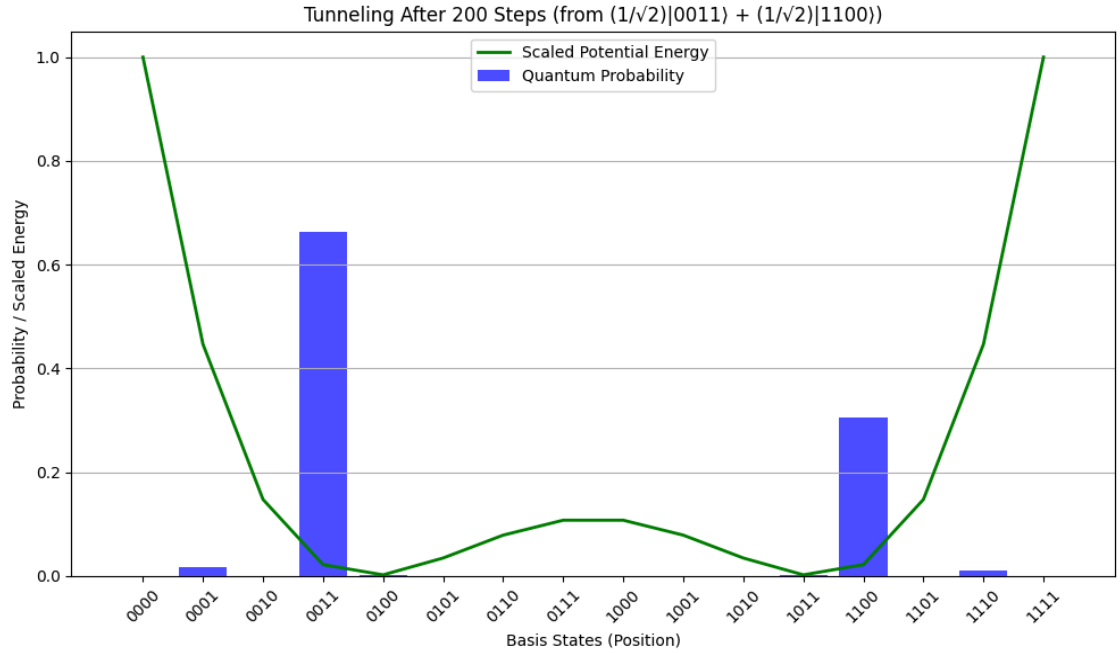

Figure 21.

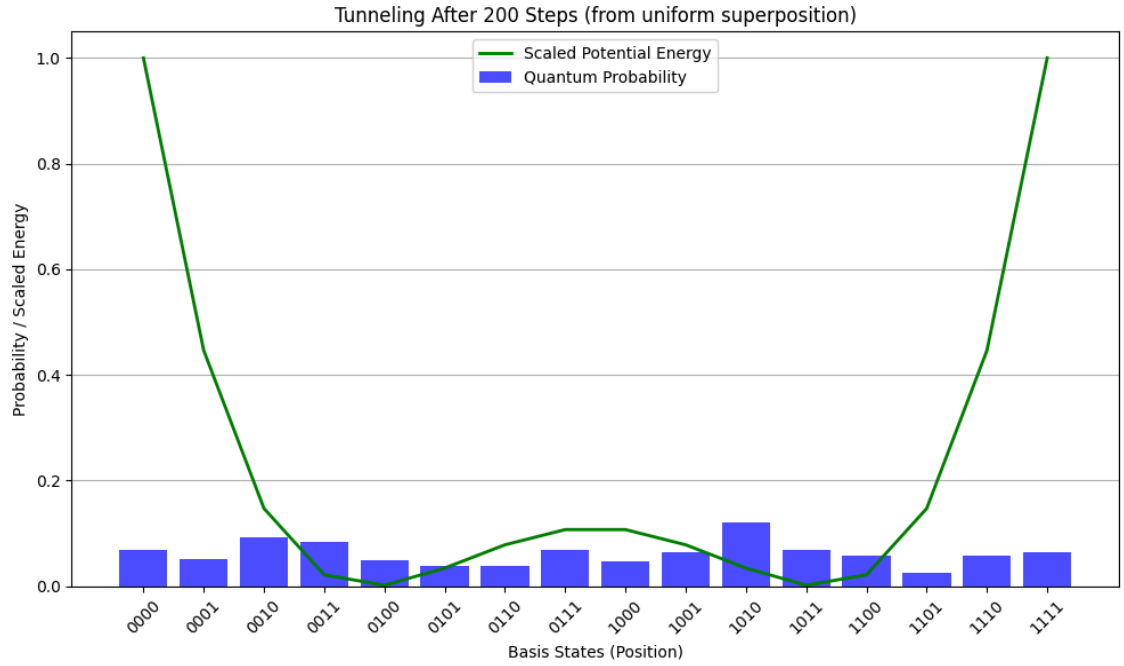

These are the results if we change the distance between the wells from 0.5 to 0.9. We can see the probabilities inside the barrier between the wells are minimal in most cases (Figure 22 - 25).

Figure 22.

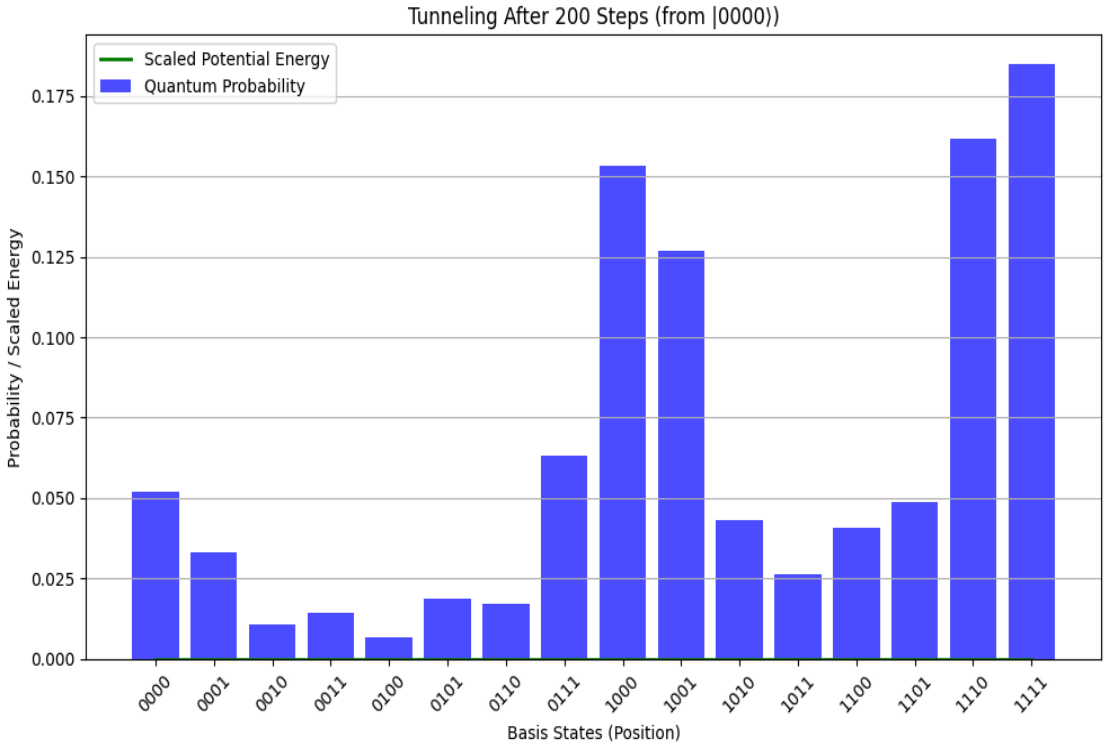

Figure 23.

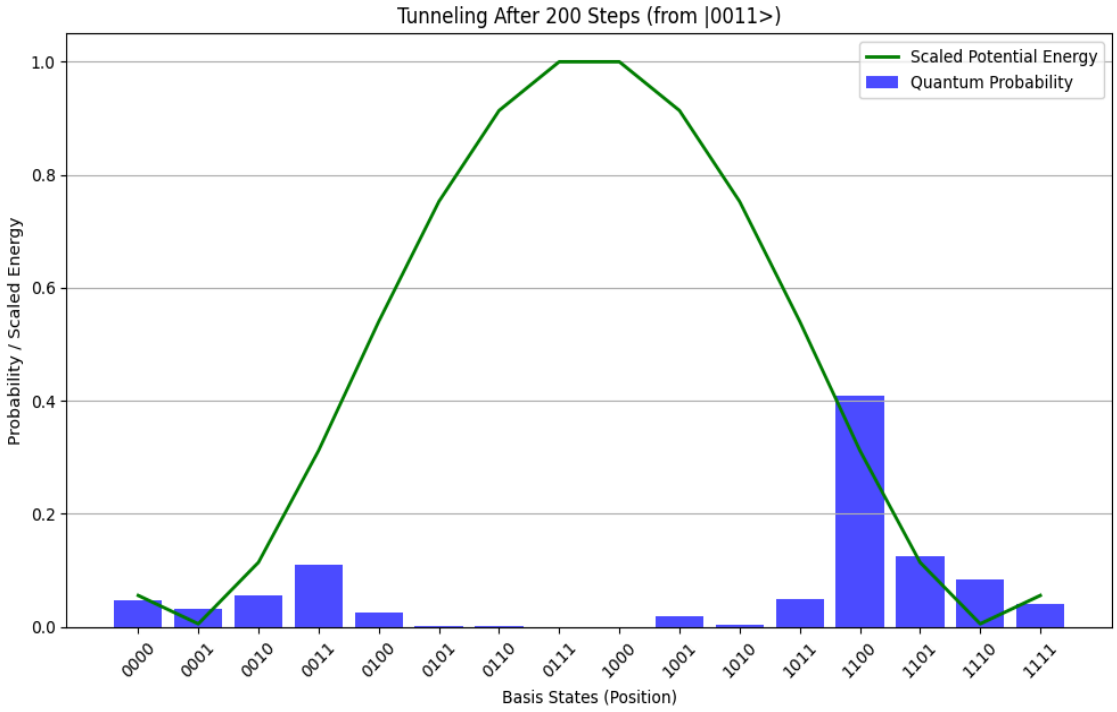

Figure 24.

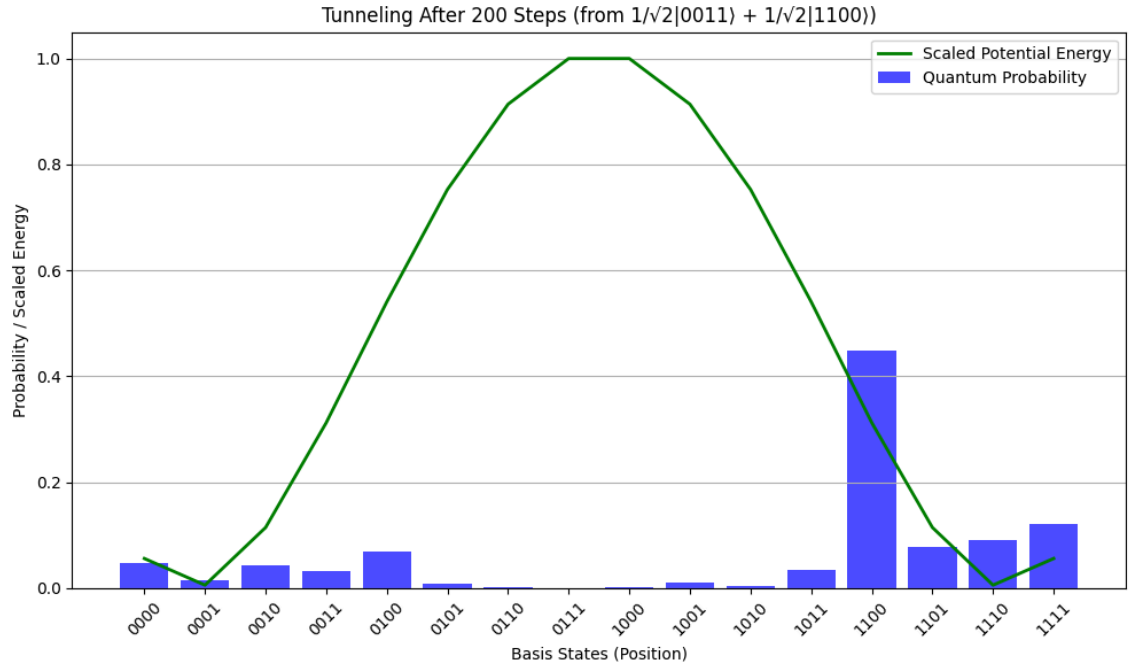

Figure 25.

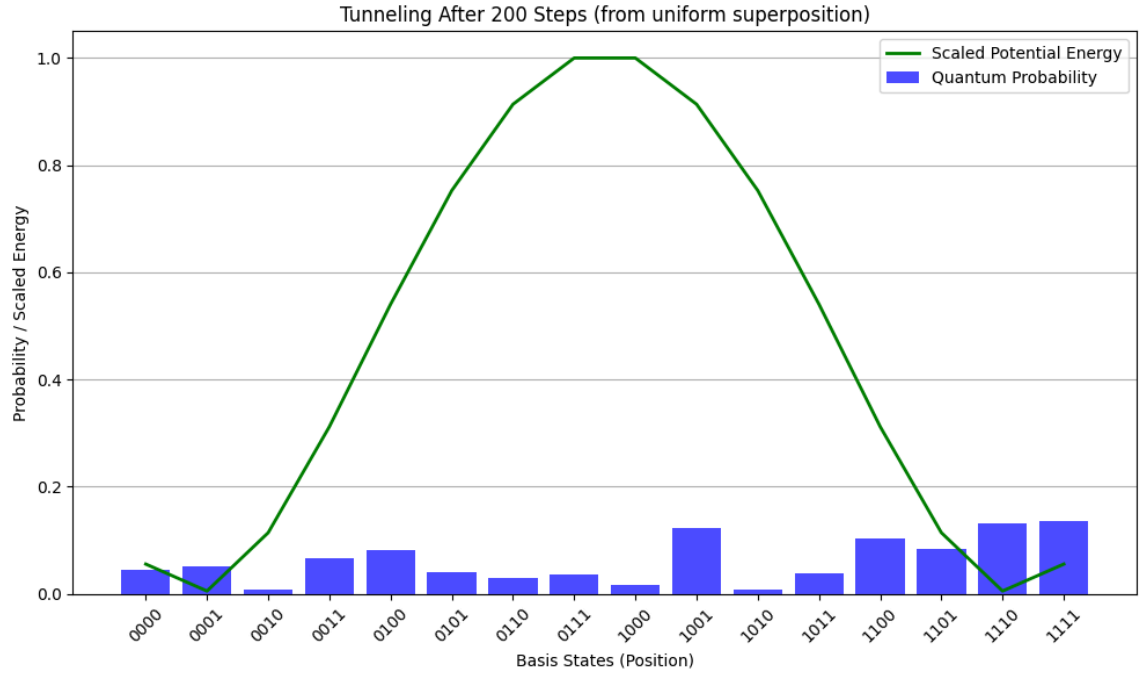

Conclusion

In this project, we successfully designed and implemented a time-evolution quantum simulation of tunneling behavior using a 4-qubit register in Qiskit. Our system mapped quantum basis states onto spatial positions along a one-dimensional lattice and evolved an initial wavefunction over time using a combination of Quantum Fourier Transforms, custom D-Gates (momentum evolution), and Q-Gates (position-based potential phase shifts). This approach allowed us to closely simulate the behavior of a quantum particle encountering different potential energy landscapes—including flat, double-well and sharply peaked barrier configurations.

Our baseline simulations (Figures 2, 3, 4, 5) confirmed that, in the absence of a potential barrier (i.e., flat V(x)), the wave function of a particle initially localized at |0000> disperses symmetrically across the position space over time. This validates the proper functioning of our kinetic evolution model, as the absence of a potential allows for free wave-like propagation driven purely by the D-Gate's momentum components.

Subsequent simulations introduced a symmetric double-well potential, characterized by the function $V(x) = a(x^2 - b^2)^2$. When we initialized the particle at the left-side well (|0011>), we observed significant tunneling behavior (Figures 6, 7, 8, 9), with probability density gradually transferring to the opposite well (|1100>) over 200 steps. This result supports the physical expectation that a particle in a bounded quantum system will non-classically penetrate through the potential barrier, a clear reflection of quantum tunneling.

To investigate quantum coherence and interference effects, we explored simulations with a superposition of left and right wells as the starting state, $\frac{1}{\sqrt{2}}(|0011 + |1100)$. These results (Figures 10, 11, 12, 13) revealed that the system undergoes intricate wavefunction interference, redistributing the probability amplitude between the wells and surrounding regions. This highlights the power of superposition and interference in enabling tunneling even from non-localized initial states.

We further evaluated a globally delocalized initial state by preparing an equal superposition across all 16 basis states. The results (Figures 14, 15, 16, 17) demonstrated that, while the initial probability distribution was uniform, the wave function naturally evolved to concentrate in the two potential wells. This aligns with quantum energy minimization, as the system transitions from a high-energy configuration into lower-energy regions—our double-well. The central barrier remained suppressed, consistent with its higher potential energy.

Finally, we examined how increasing the amplitude of the potential (the height of the barrier) affected tunneling behavior (Figures 18. 19, 20, 21). A significant increase in the parameter a from 50 to 50,000 steepened the barrier and deepened the wells, effectively reducing the particle's ability to cross the central region. The wavefunction in this regime was more localized within the wells, and tunneling became markedly less pronounced. This experiment validates the theoretical dependence of tunneling probability on barrier height and width—a well-established principle in quantum mechanics.

In total, our simulation demonstrates that even with limited qubit resolution, meaningful quantum tunneling behavior can be captured. By modulating the initial state, the potential profile, and the evolution parameters (Δt and number of steps), we were able to replicate a variety of quantum dynamics and observe rich behaviors including interference, well-to-well tunneling, and energy-driven localization.

These results validate the feasibility of simulating quantum tunneling dynamics in discrete quantum systems using low-qubit quantum ranges.

Future Work

Using this system, we can scale our number of qubits up to a maximum of 30. 30 is the maximum number of qubits that IBM's Qiskit supports. Scaling up the number of qubits will allow our simulation to represent the rotation phases of the states over time linearly and the number of possible measurements exponentially. Increasing the number of measurements will also allow us to place the wells further apart to simulate the effects of tunneling in further placed potentials.

Fine-tuning θ in each of the rotation matrices (Z, ϕ, Q) for a specific system will allow for an accurate representation of a specific particle or molecule's motion.

References

1. Feng, Guan-Ru, Yao Lu, Liang Hao, Fei-Hao Zhang, and Gui-Lu Long. “Experimental Simulation of Quantum Tunneling in Small Systems.” *Scientific Reports* 3, no. 1 (August 20, 2013): 2232. https://doi.org/10.1038/srep02232.
2. Griffiths, David J**.** *Introduction to Quantum Mechanics*. 3rd ed. Cambridge: Cambridge University Press, 2018.
3. Lloyd, Seth. “Universal Quantum Simulators.” *Science* 273, no. 5278 (1996): 1073–78. https://doi.org/10.1126/science.273.5278.1073
4. Rioux, R. (n.d.). *Basic quantum mechanics in coordinate, momentum, and phase space*. LibreTexts. Retrieved from https://chem.libretexts.org/Bookshelves/Physical_and_Theoretical_Chemistry_Textbook_Maps/Quantum_Tutorials_%28Rioux%29/01%3A_Quantum_Fundamentals/1.19%3A_Basic_Quantum_Mechanics_in_Coordinate_Momentum_and_Phase_Spacehttps://academicworks.cuny.edu/le_pubs/35/
5. Rodríguez-Sotelo, S. J., & Kozuch, S. (2025). Tunneling splitting energy vs. tunneling rate constant: An empirical computational corroboration. *Chemical Physics Letters, 864*, 141890. https://doi.org/10.1016/j.cplett.2025.141890
6. Sornborger, Andrew T. “Quantum Simulation of Tunneling in Small Systems.” *Scientific Reports* 2, no. 1 (August 22, 2012): 597. https://doi.org/10.1038/srep00597.
7. University of Texas at Austin. (n.d.). *Motion in one-dimensional potential*. Retrieved from https://farside.ph.utexas.edu/teaching/celestial/Celestial/node9.html